Oncogene (2007) 26, 7833–7846

www.nature.com/onc

ORIGINAL ARTICLE

The evolutionarily conserved EBR module of RALT/MIG6 mediates suppression of the EGFR catalytic activity

S Anastasi[1], MF Baietti[1,3], Y Frosi[1,3], S Alemà[2] and O Segatto[1]

[1]*Department of Experimental Oncology, Laboratory of Immunology, Regina Elena Cancer Institute, Rome, Italy and* [2]*Institute of Cell Biology, CNR, Monterotondo, Italy*

Physiological signalling by the epidermal growth factor receptor (EGFR) controls developmental processes and tissue homeostasis, whereas aberrant EGFR activity drives oncogenic cell transformation. Under normal conditions, the EGFR must therefore generate outputs of defined strength and duration. To this aim, cells balance EGFR activity via different modalities of negative signalling. Increasing attention is being drawn on transcriptionally controlled feedback inhibitors of EGFR, namely RALT/MIG6, LRIG1, SOCS4 and SOCS5. Genetic studies in mice have revealed the essential role of Ralt/Mig6 in regulating Egfr-driven skin morphogenesis and tumour formation, yet the mechanisms through which RALT abrogates EGFR activity are still undefined. We report that RALT suppresses EGFR function by inhibiting its catalytic activity. The evolutionarily conserved ErbB-binding region (EBR) is necessary and sufficient to carry out RALT-dependent suppression of EGFR kinase activity *in vitro* and in intact cells. The mechanism involves binding of the EBR to the 953RYLVIQ958 sequence, which is located in the αI helix of the EGFR kinase and has been shown to participate in allosteric control of EGFR catalytic activity. Our results uncover a novel mechanism of temporal regulation of EGFR activity in vertebrate organisms.
Oncogene (2007) **26,** 7833–7846; doi:10.1038/sj.onc.1210590; published online 18 June 2007

Keywords: EGFR; RALT; MIG6; feedback inhibition; negative signalling; tumour suppression

Introduction

Signal output by receptor tyrosine kinases (RTKs) is controlled via a dynamic equilibrium between mechanisms of signal generation and signal extinction. Significantly, unrestrained RTK activity may cause developmental abnormalities and post-natal pathologies such as cancer (Fiorini *et al*., 2001).

The epidermal growth factor (EGF) receptor (EGFR) has served as a paradigm model system to study mechanisms of negative signalling to RTKs. Once engaged by EGF, and concomitantly to the initiation of its signalling activity, the EGFR is rapidly removed from the cell surface. Internalized EGF:EGFR complexes are destined to be recycled to the cell surface unless sustained EGFR signalling leads to receptor ubiquitylation (Marmor and Yarden, 2004). The role of ubiquitin tags is to divert EGFR molecules to late endosomes/multivescicular bodies, thus promoting their eventual degradation in lysosomes (Marmor and Yarden, 2004; Sigismund *et al*., 2004). While recycling allows for recursive EGFR signalling (Wiley *et al*., 2003), trafficking to lysosomes results in the depletion of both ligands and receptors, ultimately leading to signal attenuation (Marmor and Yarden, 2004; Polo *et al*., 2004).

Recent studies have indicated that negative signalling to the EGFR is reinforced over time by the activity of feedback inhibitors, namely LRIG1 (Gur *et al*., 2004; Laederich *et al*., 2004), SOCS4, SOCS5 (Kario *et al*., 2005; Nicholson *et al*., 2005) and RALT (also known as MIG6 or Gene 33) (Hackel *et al*., 2001; Anastasi *et al*., 2003; Xu *et al*., 2005), which are expressed in the context of transcriptional responses triggered by EGFR itself. RALT was the first feedback inhibitor of EGFR to be discovered in mammalian cells. Its overexpression in cultured cells causes potent suppression of mitogenic and transforming signals downstream to EGFR and other ErbB RTKs (Fiorentino *et al*., 2000; Hackel *et al*., 2001; Anastasi *et al*., 2003; Xu *et al*., 2005). Conversely, loss of RALT signalling mediated by RNAi enhances the mitogenic potency of suboptimal doses of EGF. This is paralleled by amplified ERK and AKT activation as well as increased accumulation of cyclins crucial for the G_1/S transition (Anastasi *et al*., 2005; Xu *et al*., 2005). Recent genetic studies in mice have yielded results fully consistent with the notion that RALT is a physiological suppressor of EGFR signalling. Thus, *Errfi1*$^{-/-}$ (ErbB receptor feedback inhibitor 1 is the HUGO designation for the gene encoding Ralt/Mig6) mice display a highly penetrant skin phenotype characterized by abnormal proliferation of keratinocytes and enhanced carcinogenesis in skin (Ferby *et al*., 2006). This phenotype is to be

Correspondence: Dr O Segatto and S Anastasi, Laboratory of Immunology, Regina Elena Cancer Institute, via Delle Messi d'Oro, 156/158, 00158 Rome, Italy.
E-mails: segatto@ifo.it and anastasi@ifo.it
[3]These authors contributed equally to this work.
Received 23 January 2007; revised 3 May 2007; accepted 15 May 2007; published online 18 June 2007

ascribed to excess Egfr signalling, since it is rescued in the wa2/wa2 background (the *waved 2* allele encodes a hypomorphic Egf receptor, see Luetteke *et al*., 1994) and may be prevented by the administration of gefitinib, a clinically used EGFR inhibitor (Ferby *et al*., 2006). In remarkable consonance, targeted expression of a K14-*Errfi1* transgene in mouse skin (Ballaro *et al*., 2005) produced a phenotype similar to that observed in waved mice (Luetteke *et al*., 1993, 1994).

An outstanding issue is the clarification of the mechanistic basis of RALT signalling to EGFR. RALT is able to form a physical complex with ligand-activated EGFR via its EBR (ErbB binding region, Anastasi *et al*., 2003). This datum suggests that RALT may act at a receptor proximal level. A clue to a role of RALT in direct regulation of EGFR signalling comes from the recent observation that loss of RALT expression is associated with increased tyrosine phosphorylation of EGFR in both primary keratinocytes obtained from *Errfi1*$^{-/-}$ mice (Ferby *et al*., 2006) and immortal cell lines subjected to RNAi (Ballaro *et al*., 2005; Xu *et al*., 2005).

Here, we report that RALT inhibits the catalytic function of the EGFR. Binding of the EBR module to the EGFR kinase domain is necessary and sufficient to carry out RALT-mediated suppression of EGFR kinase activity *in vitro* and in intact cells. We also demonstrate structural and functional conservation of the EBR throughout the evolution of vertebrates.

Results

The EBR module of RALT inhibits the catalytic function of EGFR

Unlike LRIG1 (Gur *et al*., 2004; Laederich *et al*., 2004), SOCS4 and SOCS5 (Kario *et al*., 2005), which suppress EGFR signalling by promoting its ubiquitin-driven degradation, ectopic RALT was able to reduce CBL-dependent ubiquitylation of EGFR (data not shown). The ability of RALT to antagonize CBL function correlated with reduced autophosphorylation of the EGFR. RALT-driven suppression of EGFR autophosphorylation was dosage dependent, as also reported by Kyriakis and coworkers (Xu *et al*., 2005), and required the integrity of the EBR module (Supplementary Figure 1).

Ectopically expressed RALT inhibited to a similar extent the phosphorylation of Tyr 845, 992, 1045, 1068 and 1173 of EGFR (Figure 1a). Global inhibition of EGFR phosphorylation was sustained (Figure 1a) and could be observed over a wide range of EGF concentrations (Figure 2a). Ectopic RALT inhibited also the autophosphorylation of ERBB2 and ERBB4, whereas tyrosine phosphorylation of PDGFR was similar in control and RALT overexpressing NIH-EGFR cells (Supplementary Figure 2). The minimal EBR was mapped to aa. 323–372 (Anastasi *et al*., 2003). Ectopically expressed $RALT_{282–396}$, that is the shortest EBR containing peptide which could be expressed at satisfactory levels in mammalian cells, was sufficient to recapitulate the suppression of EGFR signalling mediated by RALT (Figure 1a), in agreement with its ability to form a ligand-dependent complex with EGFR in living cells (Figure 1b). Importantly, RALT and $RALT_{282–396}$ were capable of inhibiting EGFR activation by TGFα (Figure 2b), a ligand that renders the EGFR refractory to the suppressive activity mediated by the endocytosis/degradation pathway.

Suppression of EGFR phosphorylation by RALT and $RALT_{282–396}$ led also to robust attenuation of downstream signalling, as assessed by probing cell lysates with phospho-antibodies against activated ERKs and AKT (Figure 1a). In general, inhibition of ERK and AKT activation was stronger in cells expressing $RALT_{282–396}$, which we interpret as a reflection of the lower residual EGFR activity observed in cells expressing $RALT_{282–396}$, in comparison to those expressing full-length RALT. Some subtle differences could also be observed when comparing the kinetics of ERK and AKT activation in control and RALT/$RALT_{282–396}$ expressing cells. While AKT activation was reduced in a robust and proportional fashion at all time points, inhibition of ERK activation was less pronounced at the earliest time point of EGF stimulation (5 min). Under initial conditions, it is conceivable that the occupancy of ligand-activated EGFR molecules by either RALT or $RALT_{282–396}$ lags behind the catalytic amplification intrinsic to the RAS-ERK signalling module, thus allowing for an initial, albeit short-lived, burst of EGF-induced ERK activity.

In principle, RALT could impact EGFR autophosphorylation by either inhibiting EGFR catalytic activity or enhancing phosphate removal by phosphotyrosine phosphatases (PTPs). Inhibition of PTP activity by pervanadate, while able to potentiate EGFR autophosphorylation in control cells, did not rescue EGFR autophosphorylation in RALT overexpressing cells (data not shown). In contrast, purified recombinant glutathione *S*-transferase (GST)-RALT proteins containing an intact EBR (Figure 3a) were able to suppress

Figure 1 RALT suppresses global EGFR autophosphorylation in intact cells via its EBR module. (**a**) MYC-tagged RALT and $RALT_{282–396}$ were expressed in NIH-EGFR cells via retrovirus infection followed by puromycin selection. Control cells (PIE) were infected with empty virus. Quiescent cells were lysed either before or after stimulation at 37°C with 20 ng/ml EGF for the indicated time (minutes). Equal amounts of cell lysate were analysed by immunoblot with the indicated antibodies. Detection was by ECL coupled to autoradiography. (**b**) MYC-tagged versions of RALT and $RALT_{282–396}$ were expressed in HeLa cells via retrovirus infection followed by puromycin selection. Cells infected with empty PIE retrovirus were used as control. Cells were rendered quiescent by serum deprivation and lysed either before or after stimulation with 20 ng/ml EGF for 5 min at 37°C. Lysates were either subjected to immunoprecipitation with anti-EGFR MoAb 108 followed by immunoblot analysis with anti-EGFR and anti-MYC antibodies (left panel) or analysed directly by immunoblot (right panel). Detection was by ECL coupled to autoradiography.

the catalytic activity of purified recombinant human EGFR (aa 672–1186, henceforth referred to as EGFR) in a number of *in vitro* kinase assays (see below).

Preincubation of EGFR with a 20-fold molar excess of GST had no consequences on EGFR autophosphorylation, whereas anti-p-Tyr immunoreactivity was

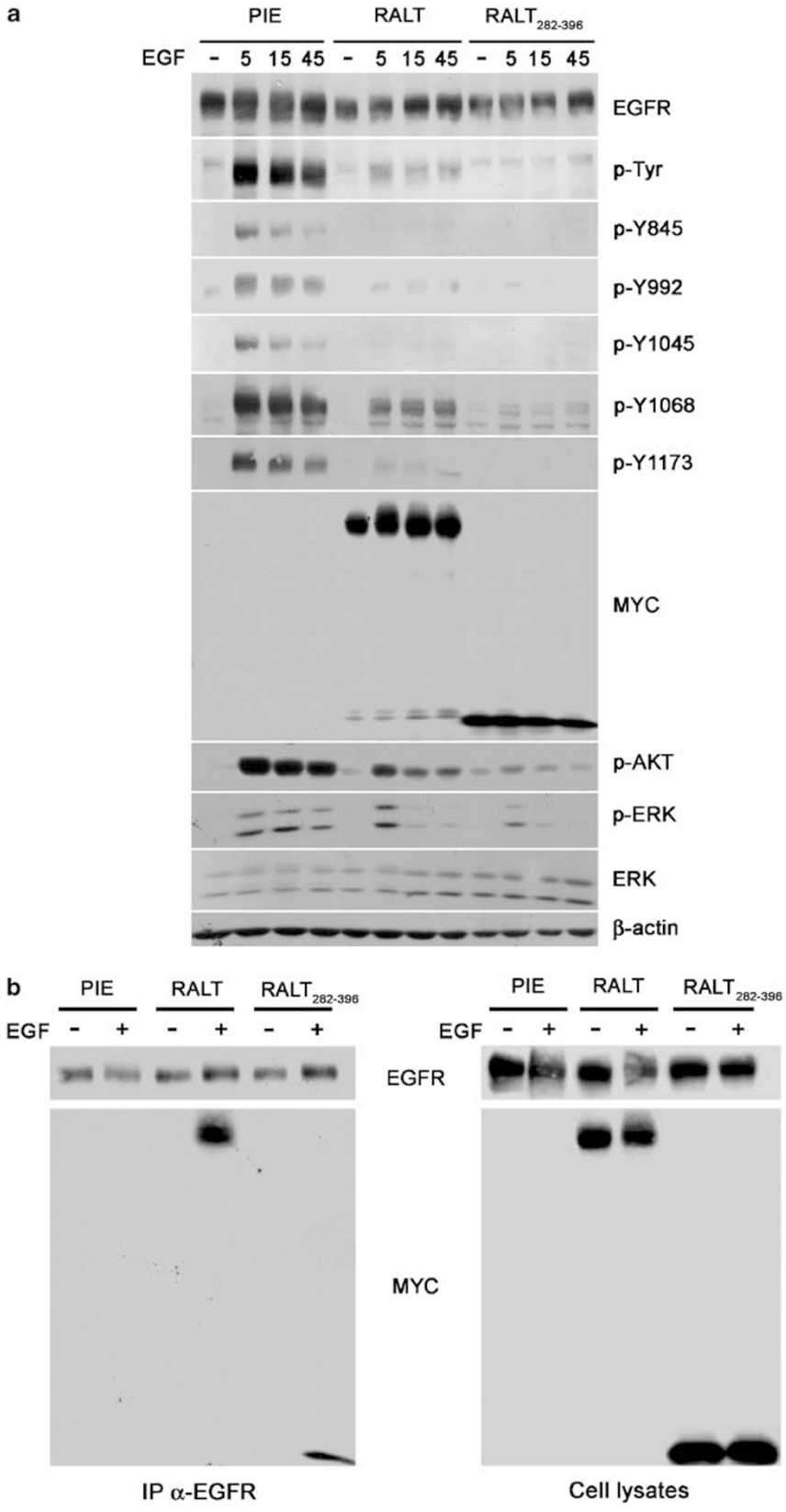

abolished in reactions containing the EGFR chemical inhibitor AG1478 (Figure 3b). Preincubation of EGFR with GST-RALT$_{282–396}$ caused a dose-dependent reduction of anti-pTyr immunoreactivity (Figure 3b), with IC_{50} values similar to those determined for the insulin receptor kinase inhibitor GRB-14 (Bereziat *et al*., 2002), and was associated to loss of reactivity with site-specific p-Tyr antibodies as well (Figure 3c). The *in vitro* autophosphorylation of EGFR was blunted also by the GST-RALT$_{262–459}$ peptide, which nevertheless lost its suppressive activity upon deletion of aa 315–361 (ΔEBR mutant) (Figures 3a and c). Recombinant peptides spanning positions 284–399 and 325–375 of human RALT (whether used as GST fusions or purified after GST tag removal) were likewise able to inhibit EGFR autophosphorylation and they did so independently of being preincubated with EGFR (not shown) or mixed with EGFR concomitantly to the start of the kinase reaction (Figure 3d). Densitometric scan of the autoradiogram shown in Figure 3d indicated that recombinant *Hs*RALT fragments suppressed EGFR autophosphorylation by about 30 and 90% when added at 4- and 16-fold molar excess over EGFR, respectively.

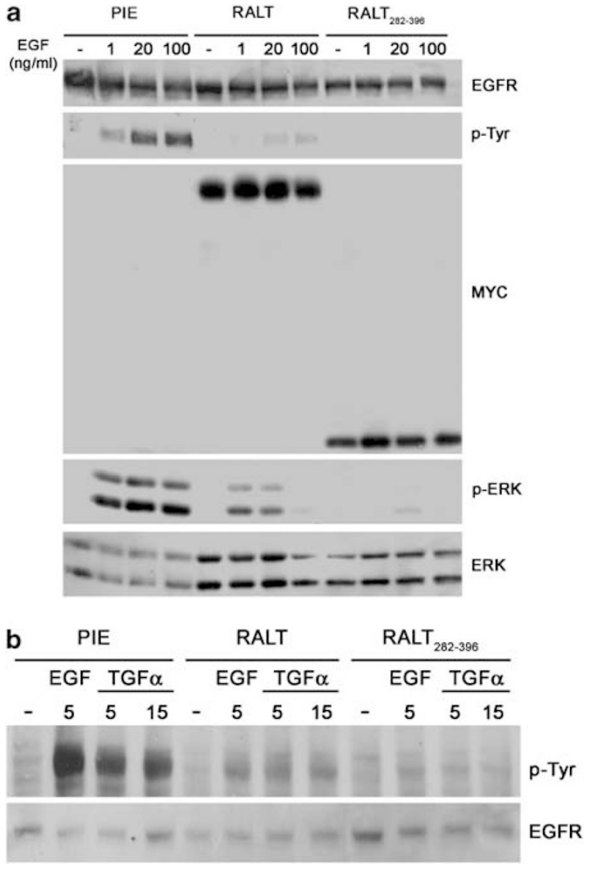

Figure 2 RALT suppresses EGFR autophosphorylation induced by TGFα and independently of EGF concentration. (**a**) Quiescent PIE, RALT and RALT$_{282–396}$ derivatives of NIH-EGFR cells were stimulated with the indicated concentrations of EGF for 5 min at 37°C. Lysates were immunoblotted with the indicated antibodies. Detection was by ECL coupled to autoradiography. (**b**) Quiescent PIE, RALT and RALT$_{282–396}$ derivatives of NIH-EGFR cells were stimulated at 37°C with either EGF (10 ng/ml for 5 min) or TGFα (50 ng/ml for 5 and 15 min). Lysates were immunoblotted with the indicated antibodies. Detection was by ECL coupled to autoradiography.

Next, we assayed the influence of RALT on EGFR-driven phosphorylation of the synthetic substrate poly (Glu,Tyr) 4:1 (PGT). As shown in Figure 4a, preincubation of GST-RALT$_{282–396}$ and GST-RALT$_{262–459}$ caused a dose-dependent reduction of phosphate incorporation into PGT, whereas neither GST nor the ΔEBR derivative of GST-RALT$_{262–459}$ were able to suppress PGT phosphorylation by EGFR. Substrate phosphorylation was suppressed also when the EGFR was allowed to undergo maximal autophosphorylation with cold ATP before the addition of GST-RALT$_{282–396}$, PGT and [γ-^{32}P]ATP to the reaction (Figure 4b). The latter experiment ruled out that inhibition of substrate phosphorylation in reactions containing GST-RALT$_{282–396}$ could be due to reduced EGFR autophosphorylation, as reported for some peptide substrates (Hsu *et al*., 1991), rather than to direct inhibition of EGFR catalytic activity.

RALT binds to the EGFR kinase domain

Tyrosine kinases show a great deal of plasticity, being subjected to tight allosteric constraints exerted by structural determinants residing in the kinase domain itself or in adjacent regulatory modules (Huse and

Figure 3 RALT EBR is necessary and sufficient to suppress EGFR autophosphorylation *in vitro*. (**a**) Schematic representation of GST fusion proteins spanning aa 282–396, 262–459 and 262–459 ΔEBR of rat (*Rn*) RALT. Full-length RALT is shown as reference. (**b**) Purified recombinant EGFR (aa 672–1186) was assayed for autophosphorylation in 1 and 5 min reactions at 25°C after 30 min preincubation with either GST or GST-RALT$_{282–396}$ at the indicated molar excess over EGFR. Controls included reactions run in the absence of GST −/+ the EGFR chemical inhibitor AG1478. Reaction products were analysed by sequential immunoblotting with anti-p-Tyr and anti-EGFR antiserum. Detection was by ECL followed by autoradiography. The top anti-p-Tyr panels were exposed for the same time, the middle panel shows a shorter exposure of the 5 min reaction. For this representative experiment the densitometric analysis of anti-p-Tyr reactivity normalized for kinase input is reported in the graph. Data are plotted as % of GST control. Variability among different experiments did not exceed 15%. (**c**) The autophosphorylation of GST-EGFR was assayed *in vitro* after a 30 min preincubation with a 20-fold molar excess of the indicated GST proteins. Reactions were run at 25°C for 5 min and products analysed by sequential immunoblotting with the indicated antibodies. Detection was by ECL coupled to autoradiography. (**d**) EGFR autophosphorylation was assayed in a 7 min reaction at 4°C. The indicated recombinant human (*Hs*) RALT proteins were mixed with EGFR simultaneously with the ATP-containing kinase reaction mix at the indicated molar ratio over EGFR. Reaction products were analysed by sequential immunoblot with the indicated antibodies. The lower panel shows a Coomassie stain of purified *Hs*RALT proteins (−/+ GST tag) used in the kinase reaction. To facilitate detection, the input of each protein was increased by 25-fold in comparison to the actual input in the kinase reaction. Molecular-weight markers were loaded in the rightmost lane.

Kuriyan, 2002). Thus, the identification of the EGFR surface necessary for RALT binding may provide insights into the mechanism underlying the EBR suppressive activity. We engineered stepwise COOH deletions of the EGFR intracellular domain and assayed these mutants for their ability to recruit RALT in co-IP

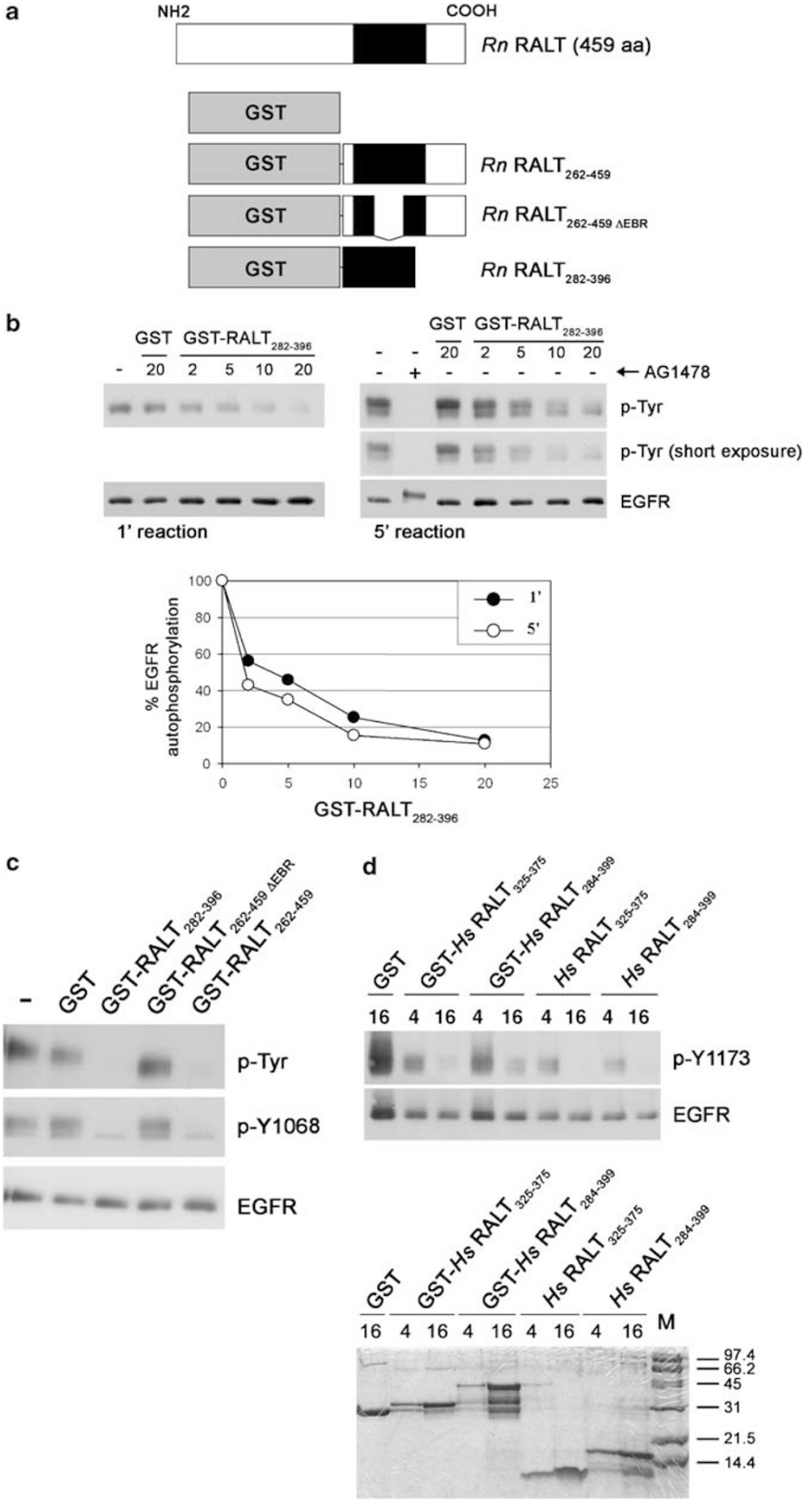

and GST pull-down assays. Cytoplasmic sequences of EGFR (Figure 5a) were fused to the dimerization domain of TPR present in the TPR-MET oncogene (Ponzetto *et al*., 1994), to mimic ligand-driven EGFR dimers. EGFR constructs extending to Q958, or beyond, were fully capable to bind RALT in intact cells (Figures

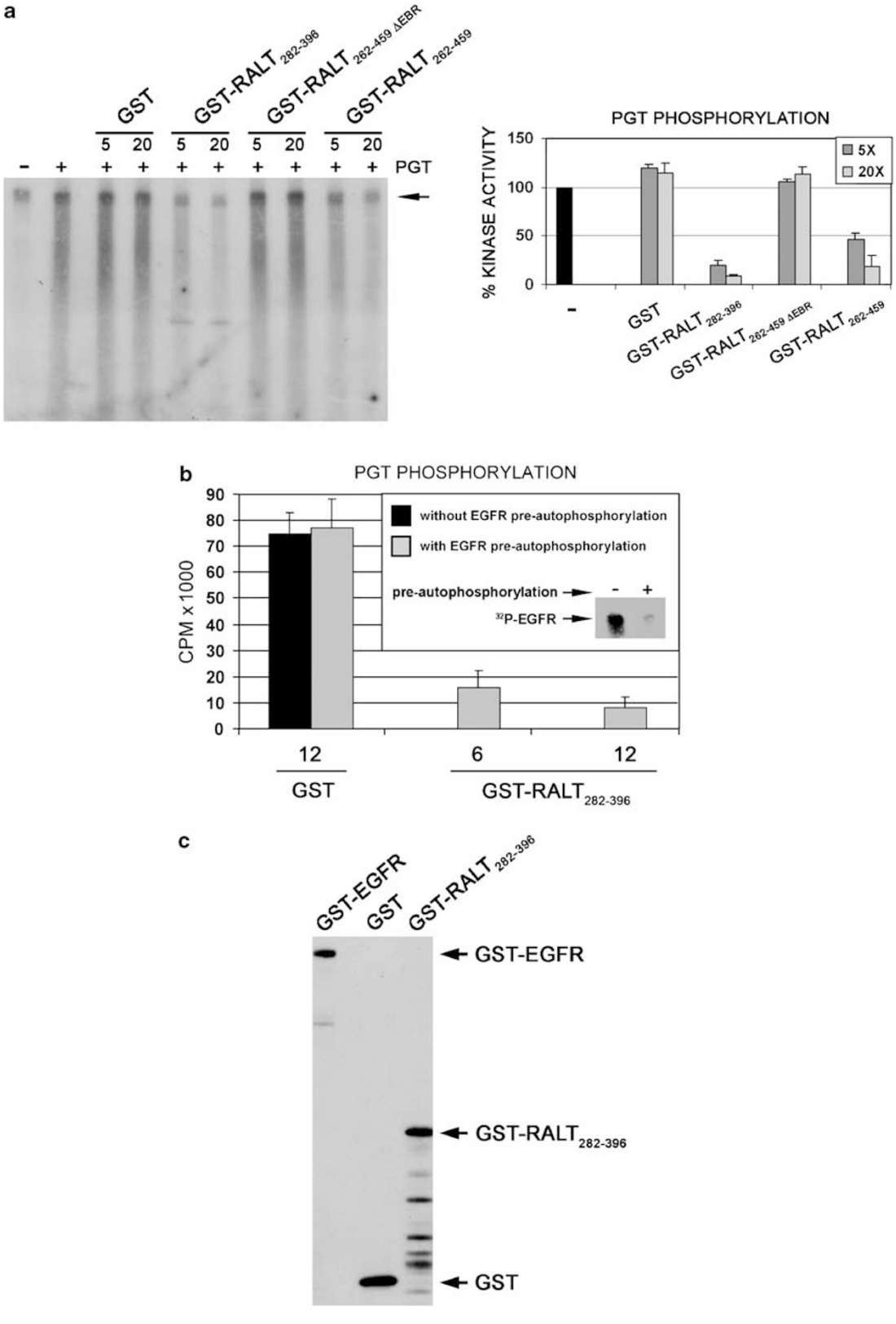

5b and c) as well as *in vitro* (Figure 5d). Premature termination at position 952 rendered the EGFR unable to complex with RALT, indicating that the 953RYLVIQ958 sequence is necessary for EGFR to bind RALT. EGFR constructs lacking the TPR sequence yielded similar results, although they bound RALT with lower efficiency (data not shown). These data are consistent with our previous finding that RALT coimmunoprecipitates with the EGFR Dc214 mutant, which terminates at position 972 (Anastasi *et al*., 2003), but are in disagreement with another report in which the EGFR 985–995 sequence was found to be necessary for the EGFR:RALT interaction, as detected in yeast 2 hybrid experiments (Hackel *et al*., 2001). To address formally whether the 985–995 sequence has any role in EGFR:RALT complex formation in mammalian cells, we engineered a TPR-EGFR construct carrying the interstitial deletion of aa. 985–995. When expressed in HEK293 cells, the 1186 Δ985–995 mutant (which can be distinguished from its 1186 wildtype counterpart due to lack of reactivity with the 1005 antibody, see Figure 6a) coimmunoprecipitated with RALT as efficiently as the TPR-EGFR 1186 and TPR-EGFR 972 constructs did (Figures 6b and c). Moreover, the 1186 Δ985–995 mutant bound to GST-$RALT_{282–396}$ with an affinity comparable to that of its wt counterpart (Figure 6d). Likewise, TPR-EGFR COOH deletion mutants in which the 985–995 sequence was either left intact (1008) or removed (972) were equally efficient in binding to GST-$RALT_{282–396}$ (Figure 6e). Thus, whether removed by a discrete interstitial deletion or a large COOH deletion, the EGFR 985–995 sequence was neither necessary to the EGFR:RALT interaction nor involved in regulating the affinity of such interaction.

The 953–958 sequence, which is conserved in all ERBB RTKs (Supplementary Figure 3), marks the COOH boundary of the αI helix of the EGFR kinase and therefore lies at the very end of the EGFR catalytic box (Stamos *et al*., 2002). Interestingly, Q958 is encoded by the most 3′ of the 32 codons of exon 24 of *EGFR*. A similar genomic organization is observed in *ERBB2*, *ERBB3* and *ERBB4* (www.ensembl.org). Thus the exon/intron organization of *ERBB* genes neatly separates the genetic information encoding the conserved catalytic boxes from that coding for the highly divergent COOH tails. We conclude that the EGFR surface involved in the interaction with the EBR is comprised in the receptor kinase domain.

The EBR is structurally and functionally conserved throughout vertebrates

Neither candidate RALT orthologs nor EBR homologous sequences are found in invertebrates. RALT appeared first in lower vertebrates and it is remarkable that the EBR region stands out as the most conserved region of RALT throughout evolution, the EBR from *D. rerio* and *Xenopus laevis* being 75 and 88% identical to that of human RALT, respectively (Supplementary Figure 4).

We expressed the two *RALT* alleles encoded by the tetraploid *X. laevis* genome (*Xl*$RALT_{401}$ and *Xl*$RALT_{404}$) in NIH-EGFR fibroblasts. Both *Xl*RALT proteins were able to form an EGF-dependent physical complex with human EGFR in co-IP assays (Supplementary Figure 5) and inhibited the autophosphorylation and downstream signalling of human EGFR (Figure 7a). The EBR module from zebrafish RALT was also able to associate with human EGFR, as assessed in GST pull-down assays (Figure 7b) and in coimmunoprecipitation experiments (Figure 7c), and to suppress EGFR kinase activity in intact cells (Figure 7c) as well as *in vitro* (Figure 7d). These data indicate that the EBR function is preserved from fish to man and that the evolutionarily most ancient EBR module is capable of suppressing the catalytic activity of human EGFR.

Discussion

The present study demonstrates that (i) RALT suppresses the catalytic activity of EGFR by binding to the EGFR kinase domain; (ii) the evolutionarily conserved EBR module is necessary and sufficient to carry out this function.

The 953RYLVIQ958 sequence of EGFR is necessary for directing the interaction of EGFR with the RALT EBR. Our data do not necessarily imply that RALT is bound by the EGFR exclusively via residues located within the 953RYLVIQ958 sequence (and/or

Figure 4 RALT EBR inhibits phosphorylation of a synthetic substrate by the EGFR kinase. (**a**) The EGFR kinase was assayed for the ability to phosphorylate the synthetic substrate poly(Glu,Tyr) 4:1 (PGT). Where indicated, reactions contained 5- or 20-fold molar excess of either GST or the indicated GST-RALT fusion proteins. Reactions were run for 5 min at 25°C in presence of [γ-^{32}P]ATP. ^{32}P incorporation into PGT was visualized by autoradiography following SDS–PAGE. Phosphorylated PGT is visualized as a smear, given the random size of PGT polymers. Note that the smear is absent in the control reaction lacking PGT. GST-EGFR undergoes autophosphorylation and is therefore labelled by ^{32}P (arrow). Smears were analysed by densitometry and PGT phosphorylation graphed as % of the control (no GST) reaction. Standard deviations among different experiments are reported in each column. (**b**) PGT phosphorylation assays were run after allowing the EGFR to undergo autophosphorylation in presence of unlabelled ATP and absence of PGT (grey columns). GST or GST-$RALT_{282–396}$ were then added to the reaction (at the indicated molar ratio over EGFR) along with PGT and fresh labelled/unlabelled ATP mixture. The dark column indicates PGT phosphorylation by non-prephosphorylated EGFR. ^{32}P incorporation into PGT was measured with a P81 filter assay coupled to scintillation counting. Standard deviations among different experiments are reported in each column. A control PGT-free reaction showed that preincubation with unlabelled ATP (+) led to stoichiometric phosphorylation of EGFR, as indicated by lack of labelling upon subsequent incubation with [γ-^{32}P]ATP (see autoradiography in the inset). (**c**) The panel shows a representative anti-GST immunoblot analysis of protein input in kinase assays, with an estimated molar excess of GST and GST-$RALT_{282–396}$ of six- and three-fold over GST-EGFR, respectively.

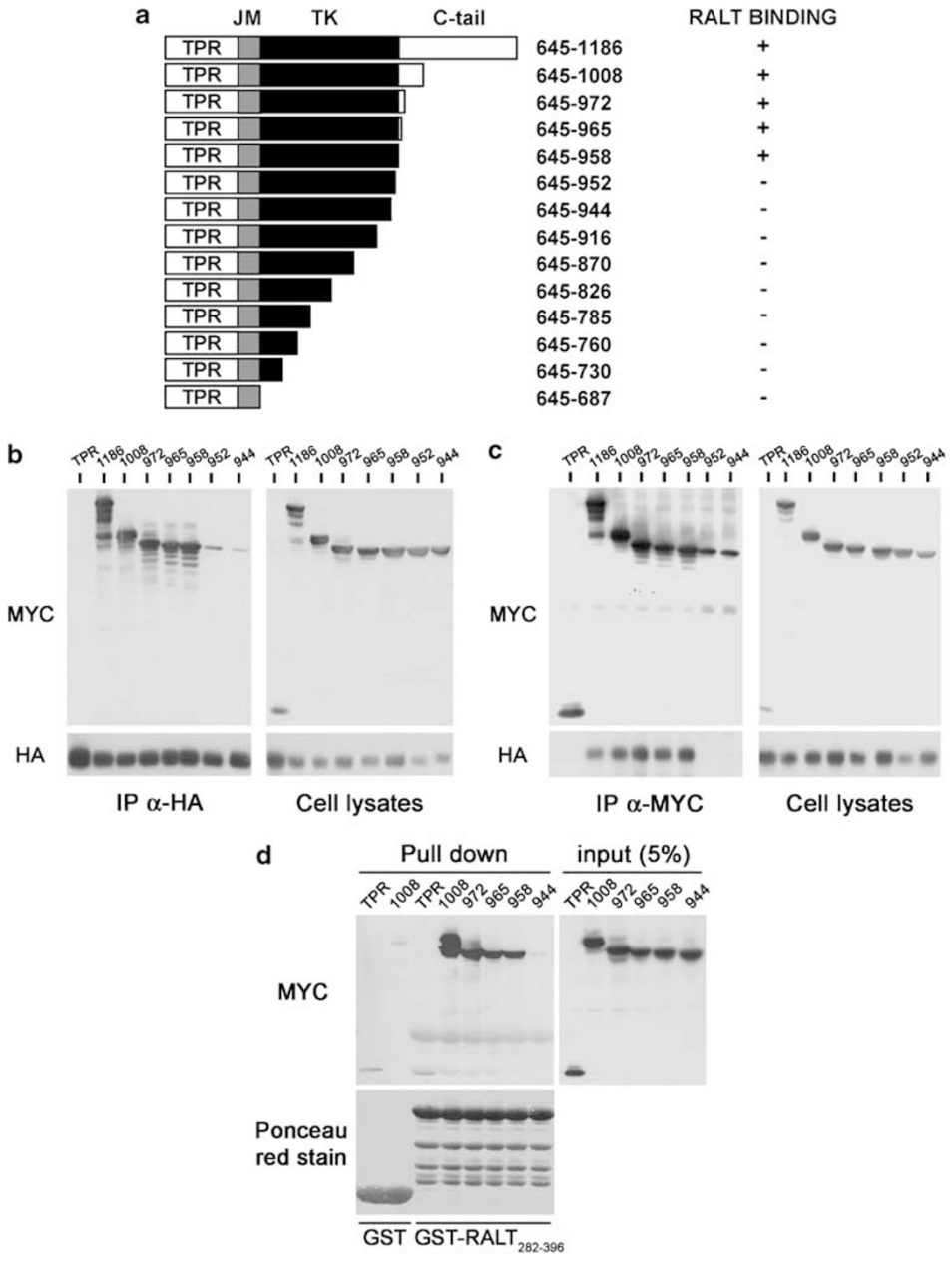

Figure 5 The EGFR surface involved in RALT recognition is comprised in the tyrosine kinase domain. (**a**) Schematic representation of TPR-EGFR constructs. EGFR sequences fused to the TPR dimerization domain comprise the juxtamembrane region (JM), the tyrosine kinase box (TK) and the COOH-terminal tail (C-tail). Numbering corresponds to residues in wt EGFR (1186 residues, accession P00533). The ability of each recombinant protein to complex with RALT in co-IP assays is reported on the right (RALT binding). (**b** and **c**) MYC-TPR or the indicated MYC-tagged TPR-EGFR chimeras were coexpressed with HA-RALT in HEK 293 cells. Lysates were subjected to immunoprecipitation with anti-HA antibody followed by anti-MYC immunoblot (**b**; upper left panel) or the reciprocal IP/WB combination (**c**, lower left panel). Filters were stripped and reprobed with the immunoprecipitating antibody (lower left panel in **b**; upper left panel in **c**). Lysates correspond to 6% of the input in immunoprecipitations (**b** and **c**, right panels). Detection was by ECL coupled to autoradiography. (**d**) TPR and the indicated TPR-EGFR fusion proteins were expressed in HEK293 cells. Lysates were incubated with purified GST or GST-RALT$_{282–396}$ immobilized onto glutathione–agarose beads. Precipitated proteins (upper left panel) and lysates corresponding to 5% of the input in binding assays (right panel) were analysed by immunoblot with anti-MYC antibodies. Loading of GST proteins in binding assays was verified by Ponceau red staining of filter (lower left panel).

immediately NH2 to it). With this caution, we note that there are several interesting features in the 953RYL-VIQ958 sequence worth to be discussed here. This motif is conserved in all ErbB family members from fish to man (data not shown), cannot be retrieved from TK sequences other than those of ErbB receptors (consistently with the notion that ErbB receptors are so far the only RTKs able to bind RALT (Fiorentino *et al*., 2000; Hackel *et al*., 2001)) and is necessary to direct also the interaction between ERBB2 and RALT in co-IP assays

(Supplementary Figure 3). Mutations of the LVI motif of ERBB3 and ERBB4, colinear to that of the 953RYLVIQ958 EGFR sequence, were found to abolish *trans*-activation of the ERBB2 kinase (Schaefer *et al*., 1999). This led to the suggestion that the LVI motif plays a crucial role in the catalytic activation of ERBB dimers (Stamos *et al*., 2002). Indeed, recent structural data support a model in which activation of the EGFR catalytic function takes place in the context of asymmetric dimers in which the COOH lobe of the catalytic domain of one receptor contacts the NH_2 lobe of the partner kinase domain, imposing to the latter a catalytically productive conformation (Zhang *et al*., 2006). Arg953 and Val956 participate in the creation of this asymmetric dimer interface (Zhang *et al*., 2006), likely explaining why mutations of the LVI motif prevent ERBB *trans*-activation (Schaefer *et al*., 1999). Within this framework, it may be proposed that, by contacting the αI helix of the EGFR kinase domain, the EBR prevents the COOH lobe from exerting its *trans*-activating function within receptor dimers. This will be formally addressed by solving the structure of the EGFR TK:EBR complex.

From the cell biology standpoint, the most relevant issue is how the EBR suppressive activity may account for the essential role of RALT in negative signalling to EGFR (Ferby *et al*., 2006) and, possibly, the entire ERBB network. In this regard, it is productive to contrast the catalytic suppression mediated by the EBR with other modalities of negative signalling to EGFR. We note that, despite its being regarded by a prevailing opinion as the major element of negative regulation of EGFR, the internalization/degradation pathway is nevertheless ineffective in several physiological scenarios. Low (<2 ng/ml), and yet biologically relevant, doses of EGF do not trigger ubiquitylation and ensuing degradation of EGFR (Sigismund *et al*., 2005). Likewise, EGFR ligands such as epiregulin (Shelly *et al*., 1998), epigen (Kochupurakkal *et al*., 2005) and TGFα (Lenferink *et al*., 1998; Longva *et al*., 2002) do not trigger receptor degradation, even at high doses. ERBB2 is refractory to endocytosis/degradation (Baulida *et al*., 1996) and may act *trans*-dominantly to inhibit the degradation of EGFR molecules recruited in EGFR. ERBB2 hetero-dimers (Lenferink *et al*., 1998; Hendriks *et al*., 2003; Haslekas *et al*., 2005). It is therefore remarkable that degradation–refractory ERBB signalling units, which are endowed with robust signalling activity (Citri and Yarden, 2006), are liable to inhibition by RALT, as exemplified by the ability of RALT to suppress (a) the autophosphorylation of EGFR activated by TGFα and low doses of EGF and (b) the autophosphorylation of ERBB2.

The added value of RALT is also evident when we place its function in the context of global feedback regulation of EGFR signalling. Here, the EBR-suppressive function emerges as an essential control element of EGFR activity in time and space. LRIG1, SOCS4 and SOCS5 inhibit EGFR by enhancing its ubiquitylation and ensuing degradation (Gur *et al*., 2004; Laederich *et al*., 2004; Kario *et al*., 2005). EGFR molecules targeted by LRIG1 and SOCS4/5 are therefore expected to retain full signalling activity until they are segregated into the degradative compartment (Miaczynska *et al*., 2004). In contrast, binding of RALT to the EGFR leads to the immediate blockade of EGFR catalytic activity. As a consequence, we envision that signalling by EGFR molecules that form a complex with RALT immediately after ligand binding is aborted at the plasmamembrane (or within its immediate proximity). Most likely, RALT is also able to bind trafficking EGFR molecules. This is relevant, since RALT becomes expressed at a time in which cells contain a sizeable population of activated EGFRs that are being routed through the endosomal compartment. The blockade of kinase activity imposed by RALT to trafficking EGFR molecules is expected to shift the kinase/PTPs equilibrium in favour of PTPs, therefore leading to a precipitous decline of pY-EGFR levels and concomitant loss of signalling competence. Consistently with this scenario, a dramatic abbreviation of the kinetics of EGFR dephosphorylation is observed in EGF stimulated cells when they are washed free of EGF and chased in presence of a pharmacological inhibitor of the EGFR kinase (Supplementary Figure 6).

Finally, it must be noted that the RALT negative feedback loop operates in the same window of time in which ErbB signalling is reinforced by positive feedback loops established by ErbB ligands, such as TGFα, whose expression is regulated at the transcriptional level by the RAS→ERK pathway (Schulze *et al*., 2001). Given that TGFα uncouples internalized EGFR molecules from degradation by driving their rapid recycling to the cell surface (Lenferink *et al*., 1998; Longva *et al*., 2002), RALT may represent the major, if not the only, means of restraining the recursive positive feedback loop generated by autocrine stimulation of the EGFR via TGFα.

Concluding remarks

The feedback inhibitors Aos and Kek1 restrain *Drosophila* EGF receptor (DER) activity by preventing the binding of ligands to DER (Shilo, 2003). We note that orthologs of Aos and Kek1 have not been identified in vertebrates and hypothesize that RALT may have evolved to preserve in vertebrates a transcriptionally controlled feedback loop dedicated to a fast termination of ErbB signalling. This function is essential, as genetic ablation of *Errfi1* leads to widespread tumourigenesis in the mouse (Ferby *et al*., 2006; Zhang *et al*., 2007). The ability of RALT to suppress the catalytic activation of ErbB RTKs may prevent cell transformation by (a) blocking ErbB signalling regardless of the type and subcellular localization of the ligand–receptor combination at work; (b) counteracting autocrine positive feedback loops that provide for robust cell activation, but have an intrinsic oncogenic potential.

Materials and methods

Materials

EGF and PDGF were from Upstate Biotechnology (Lake Placid, NY, USA), TGFα was from R&D Systems

(Minneapolis, MN, USA), tissue culture media were purchased from Cambrex (North Brunswick, NJ, USA) and sera from HyClone (Logan, UT, USA). Protein A sepharose and glutathione–agarose were from Amersham Biosciences (Piscataway, NJ, USA), DNA restriction and modifying enzymes were from New England BioLabs (Ipswich, MA, USA).

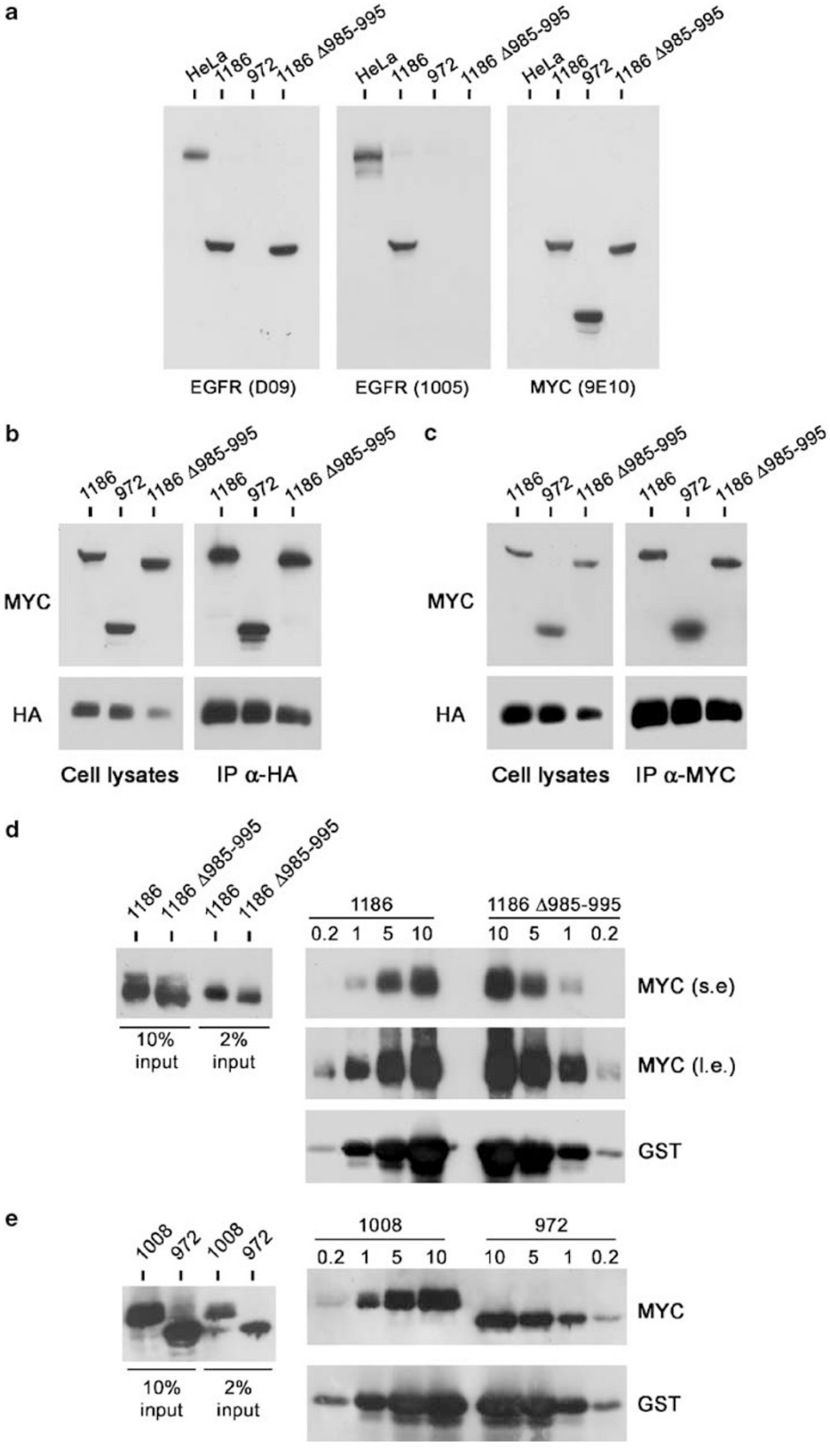

Cell culture

HeLa, HEK293, ecotropic and amphotropic Phoenix packaging cell lines were grown in Dulbecco's modified minimal essential medium (DMEM) containing 10% (v/v) foetal calf serum (FCS). To induce quiescence, cell monolayers were rinsed with phosphate-buffered solution and incubated in DMEM 0.2% FCS. NIH-EGFR, NIH-ERBB-4 (Anastasi *et al*., 2003) and NIH-EGFR/ERBB-2 cells (Di Fiore *et al*., 1990) have been described. Recombinant retrovirus stocks were generated in Phoenix cells and infections carried out as described (Fiorentino *et al*., 2000).

Immunochemical procedures

For immunoprecipitation and western blot analysis cells were lysed in ice-cold HNTG buffer (50 mM HEPES, pH 7.4, 150 mM NaCl, 10% glycerol, 5 mM EDTA, 1% Triton X-100) containing 1 mM Na_3VO_4 and a cocktail of protease inhibitors. For western blot analysis lysates were electrophoresed in sodium dodecyl sulphate–polyacrylamide gel electrophoresis (SDS–PAGE) and transferred onto nitrocellulose filters as described (Fiorentino *et al*., 2000). For immunoprecipitations monoclonal antibodies 9E10 (anti-MYC), 12CA5 (anti-HA) and 108 (anti-EGFR) were covalently coupled to protein A sepharose and used at 10–20 μg Ab/IP. Immunoprecipitations were carried out at 4°C for 3–4 h. For western blot detection, purified rabbit antibodies anti-ERK (Cell Signaling Technology, Danvers, MA, USA), anti-p-AKT (p-Ser 473, Cell Signaling), anti-EGFR C terminus (Ab 1005, Santa Cruz Biotechnology, Santa Cruz, CA, USA), anti-EGFR phosphorylated Y845, Y992, Y1045, Y1068, Y1173 (Cell Signaling Technology) were used at 2 μg/ml, anti-p-Tyr MoAb 4G10 (Upstate Biotechnology) was used at 0.5 μg/ml, monoclonal antibodies anti-MYC (9E10), anti-HA (12CA5), anti p-ERK (p-Thr 202, p-Tyr 204, Cell Signaling Technology) and anti-RALT (19C5/4) were used at 2 μg/ml. Rabbit polyclonal antiserum D09 raised against the most COOH 12 residues of human EGFR was a gift from S Polo and was used at 1:6000 dilution. Secondary HRP-conjugated antibodies were from Bio-Rad (Hercules, CA, USA). ECL detection (Amersham) was as described (Fiorentino *et al*., 2000).

In vitro *kinase assays*

Recombinant GST-EGFR (aa 672–1186) was obtained from Upstate Biotechnology. GST and GST-RALT fusion proteins were expressed and purified as described (Fiorentino *et al*., 2000). *Hs*RALT 284–399 and 325–375 were purified free of GST by digestion with Prescission protease (Amersham) according to manufacturer's recommendations. After incubating the EGFR kinase (30–50 ng/assay) with GST or GST-RALT fusions for 30 min at 4°C, kinase reactions were initiated at 25°C by adding 60 μM ATP and terminated by adding ethylenediaminetetraacetic acid (EDTA) to a final concentration of 0.1 M. Where appropriate, GST proteins were added concomitantly to the ATP mix. Reactions were run in 50 μl volume containing 8 mM MOPS, pH 7.0, 0.5 mM HEPES, pH 7.5, 0.2 mM EDTA, 200 mM $(NH_4)_2SO_4$, 10 mM $MnCl_2$, 7 mM $MgCl_2$. Poly(Glu, Tyr) 4:1 (Sigma, St Louis, MO, USA) was used at 10–30 μM. PGT phosphorylation assays contained also 10 μCi/reaction [γ-^{32}P]ATP (3000 Ci/mM, Amersham). PGT assays were analysed by either autoradiography (following SDS–PAGE) or counting c.p.m. retained on P81 filters. Background was determined by parallel processing of reactions containing all reagents, but GST-EGFR.

GST pull-down assays

GST fusion proteins were immobilized onto glutathione–agarose beads (Amersham) and incubated with cell lysates for 16 h at 4°C to detect binding at equilibrium conditions. For assaying the apparent affinities of TPR-EGFR proteins for GST-$RALT_{282–396}$, binding assays were carried out for 2 h at 4°C in a 500 μl volume. GST-$RALT_{282–396}$ was used in a 440–8.8 nM range. The input of TPR-EGFR (present in HEK293 cell lysates) was kept constant and normalized to obtain homogeneous concentrations of the different TPR-EGFR recombinant proteins.

Recombinant DNA

pcDNA3-RALT and pcDNA3-RALT ΔEBR were described (Anastasi *et al*., 2003). To obtain MYC-tagged constructs, cDNAs encoding RALT and $RALT_{282–396}$ were generated by PCR amplification and cloned downstream a 6 × MYC tag in the *Eco*RI-*Xho*I sites of the pCS2 MT vector. MYC-tagged *Bam*HI-*Xho*I inserts from pCS2 MT constructs were transferred into the retroviral pMX PIE vector. The sequence encoding the dimerization motif of TPR, corresponding to aa. 1–142 of the TPR-MET oncoprotein (accession U19348), was PCR amplified from the pMT2-TPR-MET vector (Ponzetto *et al*., 1994) and cloned into the *Eco*RI and *Xho*I sites of pCS2 MT to generate the pCS2 MT-TPR vector. Human EGFR fragments were generated by PCR amplification of a cDNA template with primers containing 5′ XhoI and 3′ *Xba*I tags. All PCR primer sequences are available upon request. PCR products were cloned in the pCS2 MT-TPR vector to generate 6 × MYC-tagged TPR-EGFR fusions. The EGFR Δ985–995 mutant was generated by cloning an *Xho*I-*Xba*I PCR fragment

Figure 6 The EGFR 985–995 sequence is dispensable for RALT binding. (**a**) Lysates from HEK293 cells expressing the indicated MYC-tagged TPR-EGFR chimeras were analysed by immunoblot with the indicated antibodies. Note that rabbit antiserum D09 (generated against a peptide corresponding to the C-terminal 12 residues of human EGFR) recognizes both TPR-EGFR 1186 and TPR-EGFR 1186 Δ985–995, whereas Santa Cruz Biotechnology antibody 1005 (raised against a peptide spanning positions 981–992) lacks reactivity against the Δ985–995 mutant, as expected. Lysates from HeLa cells were used as control for immunoreactivity against full length EGFR. (**b** and **c**). The indicated Myc-tagged TPR-EGFR chimeras were coexpressed with HA-RALT in HEK293 cells. Lysates were subjected to immunoprecipitation with anti-HA antibody followed by anti-MYC immunoblot (**b**, right panels) or the reciprocal IP/WB procedure (**c**, right panels). Filters were stripped and reprobed with the immunoprecipitating antibody. Lysates correspond to 5% of the input in immunoprecipitations (**b** and **c**, left panels). Detection was by ECL coupled to autoradiography. (**d** and **e**) Different amounts of GST-*Rn*$RALT_{282–396}$ were immobilized onto glutathione–agarose beads (10, 5, 1 and 0.2 μg, concentration range 440–8.8 nM) and incubated with extracts derived from HEK 293 cells transiently transfected to express the indicated MYC-tagged TPR-EGFR chimeras. Precipitated proteins and lysates corresponding to 2 and 10% of the input in pull-down assay were analysed by immunoblot with anti-MYC antibody. The input of GST-$RALT_{282–396}$ in pull-down assays was visualized by anti-GST antibody (GST). Detection was by ECL coupled to autoradiography. In (**d**), shorter (s.e.) and longer (l.e.) exposures of the anti-MYC autoradiography are shown.

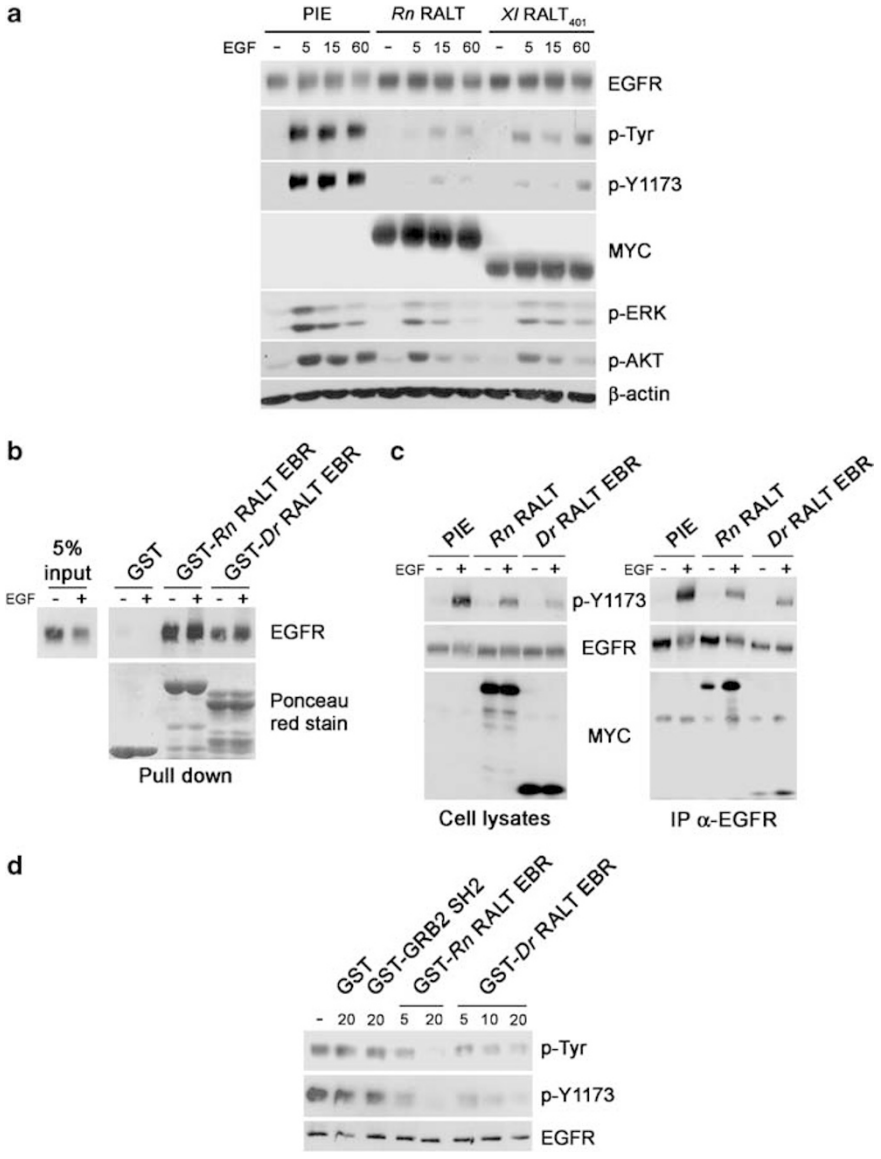

Figure 7 The RALT EBR function is conserved throughout vertebrates. (**a**) MYC-tagged *Rn*RALT and *Xl*RALT$_{401}$ (*Xenopus laevis*) were expressed in NIH-EGFR cells via retrovirus infection followed by puromycin selection. PIE cells were used as control. Quiescent monolayers were lysed before or after stimulation with 20 ng/ml EGF at 37°C for the indicated time (minutes). Equal amounts of cell lysate were immunoblotted with the indicated antibodies. Note that *Xl*RALT$_{401}$ is 58 aa smaller than *Rn*RALT and therefore migrates faster in SDS–PAGE. (**b**) GST, GST-*Rn*RALT EBR and GST-*Dr*RALT EBR (*Dr*RALT EBR corresponds to the *Danio rerio* RALT sequence aligning with aa. 282–396 of *Rn*RALT, see Supplementary Figure 4) were purified onto glutathione–agarose beads and incubated with extracts obtained from quiescent HeLa cells stimulated for 5 min at 37°C with either carrier or 20 ng/ml EGF. Precipitated proteins and lysates corresponding to 5% of the input in binding assays were analysed by immunoblot with anti-EGFR antibodies. Detection was by ECL followed by autoradiography. Loading of GST proteins in binding assays was verified by staining the filter with Ponceau red (lower panel). (**c**) The EBR module of *Dr*RALT was expressed in NIH-EGFR cells as 6 × MYC fusion using retrovirus infection followed by puromycin selection. PIE and *Rn*RALT cells were used as controls. Lysates (left panel) and anti-EGFR immunoprecipitates (right panel) were probed with the indicated antibodies. Detection was by ECL followed by autoradiography. (**d**) The indicated purified GST fusion proteins were mixed with purified recombinant EGFR at the indicated molar excess. Kinase reactions were run for 5 min at 25°C and sequentially immunoblotted with the indicated antibodies. Detection was by ECL coupled to autoradiography.

corresponding to aa 996–1186 into pCS2 MT-TPR. An *Xho*I-*Xho*I PCR product (aa 645–984) was then joined to the above *Xho*I-*Xba*I fragment to generate the Δ985–995 construct. In this construct the LE sequence generated by the novel *Xho*I site used to engineer the mutation replaces the 985DVVDADEY-LIP995 sequence of wt EGFR.

GST-RALT$_{262–459}$ and GST-RALT$_{282–396}$ have been described (Fiorentino *et al*., 2000). GST-RALT$_{262–459}$ ΔEBR was generated by cloning an *Eco*RV-*Xho*I fragment from pcDNA3-RALT$_{\Delta EBR}$ into pGEX 4T1. GST-*Hs*RALT 284–399 and 325–375 were generated by cloning PCR amplified fragments into the *Bam*HI and *Sal*I sites of pGEX6p-2RBS (obtained from A Musacchio).

Acknowledgements

We thank V Federici for ERBB2/RALT co-IP studies, M Fanciulli, C Gaetano, A Musacchio, S Giordano, P Pisu, S Polo, Y Yarden and A Zingoni for reagents, PG Natali for support, L Sibilio for help with PDB analysis and R Fraioli for antibody purification. OS is supported by MIUR-FIRB, the Italian Ministry of Health and AIRC. S Alemà is supported by MIUR-FIRB and AIRC.

References

Anastasi S, Fiorentino L, Fiorini M, Fraioli R, Sala G, Castellani L *et al*. (2003). Feedback inhibition by RALT controls signal output by the ErbB network. *Oncogene* **22**: 4221–4234.

Anastasi S, Sala G, Huiping C, Caprini E, Russo G, Iacovelli S *et al*. (2005). Loss of RALT/MIG-6 expression in ERBB2-amplified breast carcinomas enhances ErbB-2 oncogenic potency and favors resistance to Herceptin. *Oncogene* **28**: 4540–4548.

Ballaro C, Ceccarelli S, Tiveron C, Tatangelo L, Salvatore AM, Segatto O *et al*. (2005). Targeted expression of RALT in mouse skin inhibits epidermal growth factor receptor signalling and generates a waved-like phenotype. *EMBO Rep* **6**: 755–761.

Baulida J, Kraus MH, Alimandi M, Di Fiore PP, Carpenter G. (1996). All ErbB receptors other than the epidermal growth factor receptor are endocytosis impaired. *J Biol Chem* **271**: 5251–5257.

Bereziat V, Kasus-Jacobi A, Perdereau D, Cariou B, Girard J, Burnol AF. (2002). Inhibition of insulin receptor catalytic activity by the molecular adapter Grb14. *J Biol Chem* **277**: 4845–4852.

Citri A, Yarden Y. (2006). EGF-ERBB signalling: towards the systems level. *Nat Rev Mol Cell Biol* **7**: 505–516.

Di Fiore PP, Segatto O, Taylor WG, Aaronson SA, Pierce JH. (1990). EGF receptor and erbB-2 tyrosine kinase domains confer cell specificity for mitogenic signaling. *Science* **248**: 79–83.

Ferby I, Reschke M, Kudlacek O, Knyazev P, Pante G, Amann K *et al*. (2006). Mig6 is a negative regulator of EGF receptor-mediated skin morphogenesis and tumor formation. *Nat Med* **12**: 568–573.

Fiorentino L, Pertica C, Fiorini M, Talora C, Crescenzi M, Castellani L *et al*. (2000). Inhibition of ErbB-2 mitogenic and transforming activity by RALT, a mitogen-induced signal transducer which binds to the ErbB-2 kinase domain. *Mol Cell Biol* **20**: 7735–7750.

Fiorini M, Alimandi M, Fiorentino L, Sala G, Segatto O. (2001). Negative regulation of receptor tyrosine kinase signals. *FEBS Lett* **490**: 132–141.

Gur G, Rubin C, Katz M, Amit I, Citri A, Nilsson J *et al*. (2004). LRIG1 restricts growth factor signaling by enhancing receptor ubiquitylation and degradation. *EMBO J* **23**: 3270–3281.

Hackel PO, Gishizky M, Ullrich A. (2001). Mig-6 is a negative regulator of the epidermal growth factor receptor signal. *Biol Chem* **382**: 1649–1662.

Haslekas C, Breen K, Pedersen KW, Johannessen LE, Stang E, Madshus IH. (2005). The inhibitory effect of ErbB2 on epidermal growth factor-induced formation of clathrin-coated pits correlates with retention of epidermal growth factor receptor-ErbB2 oligomeric complexes at the plasma membrane. *Mol Biol Cell* **16**: 5832–5842.

Hendriks BS, Opresko LK, Wiley HS, Lauffenburger D. (2003). Coregulation of epidermal growth factor receptor/human epidermal growth factor receptor 2 (HER2) levels and locations: quantitative analysis of HER2 overexpression effects. *Cancer Res* **63**: 1130–1137.

Hsu CY, Hurwitz DR, Mervic M, Zilberstein A. (1991). Autophosphorylation of the intracellular domain of the epidermal growth factor receptor results in different effects on its tyrosine kinase activity with various peptide substrates. Phosphorylation of peptides representing Tyr(P) sites of phospholipase C-gamma. *J Biol Chem* **266**: 603–608.

Huse M, Kuriyan J. (2002). The conformational plasticity of protein kinases. *Cell* **109**: 275–282.

Kario E, Marmor MD, Adamsky K, Citri A, Amit I, Amariglio N *et al*. (2005). Suppressors of cytokine signaling 4 and 5 regulate epidermal growth factor receptor signaling. *J Biol Chem* **280**: 7038–7048.

Kochupurakkal BS, Harari D, Di Segni A, Maik-Rachline G, Lyass L, Gur G *et al*. (2005). Epigen, the last ligand of ErbB receptors, reveals intricate relationships between affinity and mitogenicity. *J Biol Chem* **280**: 8503–8512.

Laederich MB, Funes-Duran M, Yen L, Ingalla E, Wu X, Carraway III KL *et al*. (2004). The leucine-rich repeat protein LRIG1 is a negative regulator of ErbB family receptor tyrosine kinases. *J Biol Chem* **279**: 47050–47056.

Lenferink AE, Pinkas-Kramarski R, van de Poll ML, van Vugt MJ, Klapper LN, Tzahar E *et al*. (1998). Differential endocytic routing of homo- and hetero-dimeric ErbB tyrosine kinases confers signaling superiority to receptor heterodimers. *EMBO J* **17**: 3385–3397.

Longva KE, Blystad FD, Stang E, Larsen AM, Johannessen LE, Madshus IH. (2002). Ubiquitination and proteasomal activity is required for transport of the EGF receptor to inner membranes of multivesicular bodies. *J Cell Biol* **156**: 843–854.

Luetteke NC, Phillips HK, Qiu TH, Copeland NG, Earp HS, Jenkins NA *et al*. (1994). The mouse waved-2 phenotype results from a point mutation in the EGF receptor tyrosine kinase. *Genes Dev* **8**: 399–413.

Luetteke NC, Qiu TH, Peiffer RL, Oliver P, Smithies O, Lee DC. (1993). TGF alpha deficiency results in hair follicle and eye abnormalities in targeted and waved-1 mice. *Cell* **73**: 263–278.

Marmor MD, Yarden Y. (2004). Role of protein ubiquitylation in regulating endocytosis of receptor tyrosine kinases. *Oncogene* **23**: 2057–2070.

Miaczynska M, Pelkmans L, Zerial M. (2004). Not just a sink: endosomes in control of signal transduction. *Curr Opin Cell Biol* **16**: 400–406.

Nicholson SE, Metcalf D, Sprigg NS, Columbus R, Walker F, Silva A *et al*. (2005). Suppressor of cytokine signaling (SOCS)-5 is a potential negative regulator of epidermal growth factor signaling. *Proc Natl Acad Sci USA* **102**: 2328–2333.

Polo S, Pece S, Di Fiore PP. (2004). Endocytosis and cancer. *Curr Opin Cell Biol* **16**: 156–161.

Ponzetto C, Bardelli A, Zhen Z, Maina F, dalla ZP, Giordano S *et al*. (1994). A multifunctional docking site mediates signaling and transformation by the hepatocyte growth factor/scatter factor receptor family. *Cell* **77**: 261–271.

Schaefer G, Akita RW, Sliwkowski MX. (1999). A discrete three-amino acid segment (LVI) at the C-terminal end of kinase-impaired ErbB3 is required for transactivation of ErbB2. *J Biol Chem* **274**: 859–866.

Schulze A, Lehmann K, Jefferies HB, McMahon M, Downward J. (2001). Analysis of the transcriptional program induced by Raf in epithelial cells. *Genes Dev* **15**: 981–994.

Shelly M, Pinkas-Kramarski R, Guarino BC, Waterman H, Wang LM, Lyass L *et al*. (1998). Epiregulin is a potent pan-ErbB ligand that preferentially activates heterodimeric receptor complexes. *J Biol Chem* **273**: 10496–10505.

Shilo BZ. (2003). Signaling by the Drosophila epidermal growth factor receptor pathway during development. *Exp Cell Res* **284**: 140–149.

Sigismund S, Polo S, Di Fiore PP. (2004). Signaling through monoubiquitination. *Curr Top Microbiol Immunol* **286**: 149–185.

Sigismund S, Woelk T, Puri C, Maspero E, Tacchetti C, Transidico P *et al*. (2005). Clathrin-independent endocytosis of ubiquitinated cargos. *Proc Natl Acad Sci USA* **102**: 2760–2765.

Stamos J, Sliwkowski MX, Eigenbrot C. (2002). Structure of the epidermal growth factor receptor kinase domain alone and in complex with a 4-anilinoquinazoline inhibitor. *J Biol Chem* **277**: 46265–46272.

Wiley HS, Shvartsman SY, Lauffenburger DA. (2003). Computational modeling of the EGF-receptor system: a paradigm for systems biology. *Trends Cell Biol* **13**: 43–50.

Xu D, Makkinje A, Kyriakis JM. (2005). Gene 33 is an endogenous inhibitor of epidermal growth factor (EGF) receptor signaling and mediates dexamethasone-induced suppression of EGF function. *J Biol Chem* **280**: 2924–2933.

Zhang X, Gureasko J, Shen K, Cole PA, Kuriyan J. (2006). An allosteric mechanism for activation of the kinase domain of epidermal growth factor receptor. *Cell* **125**: 1137–1149.

Zhang YW, Staal B, Su Y, Swiatek P, Zhao P, Cao B *et al*. (2007). Evidence that MIG-6 is a tumor-suppressor gene. *Oncogene* **26**: 269–276.

Supplementary Information accompanies the paper on the Oncogene website (http://www.nature.com/onc).